A fluorophore attached to nicotinic acetylcholine receptor βM2 detects productive binding of agonist to the αδ site

David S. Dahan*, Mohammed I. Dibas‡, E. James Petersson*, Vincent C. Auyeung‡, Baron Chanda§, Francisco Bezanilla§, Dennis A. Dougherty*, and Henry A. Lester‡¶

Divisions of *Chemistry and Chemical Engineering and ‡Biology, 1200 East California Boulevard, California Institute of Technology, Pasadena, CA 91125; and §Department of Physiology and Department of Anesthesiology, David Geffen School of Medicine, University of California, Los Angeles, CA 90095

Edited by Arthur Karlin, Columbia University College of Physicians and Surgeons, New York, NY, and approved April 19, 2004 (received for review April 1, 2003)

To study conformational transitions at the muscle nicotinic acetylcholine (ACh) receptor (nAChR), a rhodamine fluorophore was tethered to a Cys side chain introduced at the β19′ position in the M2 region of the nAChR expressed in *Xenopus* oocytes. This procedure led to only minor changes in receptor function. During agonist application, fluorescence increased by ($\Delta F/F$) ≈10%, and the emission peak shifted to lower wavelengths, indicating a more hydrophobic environment for the fluorophore. The dose–response relations for ΔF agreed well with those for epibatidine-induced currents, but were shifted ≈100-fold to the left of those for ACh-induced currents. Because (*i*) epibatidine binds more tightly to the αγ-binding site than to the αδ site and (*ii*) ACh binds with reverse-site selectivity, these data suggest that ΔF monitors an event linked to binding specifically at the αδ-subunit interface. In experiments with flash-applied agonists, the earliest detectable ΔF occurs within milliseconds, i.e., during activation. At low [ACh] (≤ 10 μM), a phase of ΔF occurs with the same time constant as desensitization, presumably monitoring an increased population of agonist-bound receptors. However, recovery from ΔF is complete before the slowest phase of recovery from desensitization (time constant ≈250 s), showing that one or more desensitized states have fluorescence like that of the resting channel. That conformational transitions at the αδ-binding site are not tightly coupled to channel activation suggests that sequential rather than fully concerted transitions occur during receptor gating. Thus, time-resolved fluorescence changes provide a powerful probe of nAChR conformational changes.

The muscle nicotinic acetylcholine receptor (nAChR) is a well studied member of the Cys-loop family of neurotransmitter-gated ion channels. A 4.6-Å structure (1) shows five ≈160-Å-long rod-shaped subunits surrounding a central channel. From the extracellular side the subunits have a counterclockwise order of αγαδβ (2, 3). Each subunit has a large extracellular N-terminal or ligand-binding domain followed by four transmembrane regions, M1–M4 (4). The structure of the extracellular ligand-binding sites, at the αγ and αδ interfaces, resembles that of a homologous molluscan ACh-binding protein (3). Numerous biochemical and electrophysiological experiments indicate that M2 lines the channel (5).

The nAChR exists in at least four distinct, interconvertible conformational states: resting, open, fast-onset-desensitized, and slow-onset-desensitized (6). The open and the fast-onset-desensitized states presumably have moderate affinity for ACh, are metastable (on millisecond time scales), and are present in low concentrations at equilibrium. The supralinear dose–response relation (Hill coefficient >1) suggests that the open state of the channel is much more likely to be associated with the presence of two bound agonist molecules than with a single bound agonist (7). In the prevailing kinetic scheme, receptors in the resting state bind two agonist molecules, isomerize to the open state, and in the continued presence of agonist, desensitize. After removal of agonist, the agonist–receptor complex dissociates and the channel closes within milliseconds; but desensitized receptors isomerize more slowly to the resting state (tens of milliseconds to hundreds of seconds). Thermodynamic considerations suggest that the resting state has low affinity for agonist, whereas the slow-onset-desensitized state is the most stable state in the presence of agonist because of its high affinity.

Kinetic analyses of single-channel and macroscopic function suggests that in the resting state, the affinity of ACh for the two sites differs by a factor of 30 (8). Experiments with partially assembled αγ and αδ dimers or with fully assembled, pentameric γ-less or δ-less receptors show that the αδ site has the higher affinity for ACh or carbamylcholine (9–11). Interestingly, epibatidine binds with 75-fold higher affinity to the αγ site (10).

To learn more about the changes in state and/or conformation, one requires a structural probe that reveals changes in real time as receptors proceed through electrophysiologically defined states. Covalently bound fluorescent probes have proven useful for this purpose at other ion channels and, recently, for γ-aminobutyric acid type C receptors as well (12). We have now covalently modified a Cys at the extracellular end of M2 with a thiol-reactive fluorophore, and we report fluorescence changes during receptor activation and desensitization. This report begins the analysis of these changes.

Materials and Methods

Reagents and Solutions. The fluorescent dye sulforhodamine methanethiosulfonate (MTSR) and the blocking reagent Na (2-sulfonatoethyl) methanethiosulfonate were purchased from Toronto Research Chemicals. The photoisomerizable agonist 3,3′-bis-[α-(trimethylammonium)methyl]azobenzene (Bis-Q) was prepared (13). Other reagents, including (±)-epibatidine, were purchased from Sigma. The full-Na recording solution, ND-96, contained 96 mM NaCl, 2 mM KCl, 1 mM $MgCl_2$, and 5 mM Hepes (pH 7.4). For low-Na recording solution, NaCl was partially replaced with equimolar *N*-methyl-D-glucamine. The incubation solution contained ND-96 solution plus 1.8 mM $CaCl_2$, 0.6 mM theophylline, 2.5 mM pyruvic acid, 50 μg/ml gentamycin, and 5% horse serum.

Molecular Biology. A pSP64T construct encoding the nAChR β-subunit with an A272C mutation (the βM2 19′ position) was obtained from A. Karlin. A 714-bp *Bst*EII/*Bsp*EI fragment was transferred to the corresponding site of a pAMV construct

This paper was submitted directly (Track II) to the PNAS office.

Abbreviations: ACh, acetylcholine; nAChR, nicotinic ACh receptor; Bis-Q, 3,3′-bis-[α-(trimethylammonium)methyl]azobenzene; MTSR, sulforhodamine methanethiosulfonate; β19′C, βA19′C nAChR.

¶To whom correspondence should be addressed. E-mail: lester@caltech.edu.

encoding the wild-type β-subunit. Capped mRNA for the embryonic mouse muscle nAChR subunits were prepared by *in vitro* runoff transcription (Ambion mMagic mMessage).

Oocyte Preparation and mRNA Injection. Stage VI oocytes of *Xenopus laevis* were harvested (14) and injected with 30 ng of mRNA at a subunit ratio 2:1:1:1 α:β:γ:δ. To achieve the high levels of expression required for detection of the fluorescent label over the background fluorescence (caused by oocyte autofluorescence and by nonspecific binding of dye), oocytes were incubated for 6–8 days at 18°C.

Fluorescent Labeling. Oocytes were rinsed and then reacted with 10 mM Na (2-sulfonatoethyl) methanethiosulfonate for 90 s to block endogenous surface sulfhydryl groups, terminated by 5 mg/ml BSA. Cys at the βM2 19′ position does not react with Na (2-sulfonatoethyl) methanethiosulfonate (15). After a wash, the oocytes were labeled with 5 μM MTSR plus 100 μM ACh for 45 s, terminated by a 5 mg/ml BSA solution. BSA, Na (2-sulfonatoethyl) methanethiosulfonate, and MTSR reagents were made up in ND-96 just before use, and all steps were performed on ice. Labeled oocytes were stored in incubating solution at 4°C for up to 72 h after labeling.

Spectral Analysis. Emission spectra from oocytes were obtained with a spectrograph and intensified charge-coupled device camera combination as described (16). Excitation filter was 535DF35, dichroic mirror was 565DRLP; no emission filter was used. Emission spectra of free MTSR dissolved in ethanol and ND98 were obtained with an SLM-Aminco fluorometer (SLM Instruments, Urbana, IL).

Simultaneous Recording of Current and Fluorescence Intensity. In the inverted fluorescence microscope fitted with a high-Q tetramethylrhodamine isothiocyanate filter set (Chroma Technology, Rockingham, VT), a 40× objective lens (N.A. 0.7, working distance 510 μm), and a photomultiplier tube (R928P, Photon Technology International, Lawrenceville, NJ) (17), a black block ≈0.4 mm high bearing a vertical slit 0.75 mm wide exposed the animal pole of the oocyte to both the perfusion solution and the beam from the 100-W Hg lamp (17). This arrangement allowed efficient perfusion of nearly the entire oocyte surface, including the optically monitored area at the top of the slit.

Two-electrode voltage clamp procedures were used (GeneClamp 500, Axon Instruments). The holding potential was −80 mV (ACh recordings) or −60 mV (epibatidine recordings). With ND-96, the average 1-μM ACh response of a batch of oocytes expressing βA19′C nAChR (β19′C) was 200–1,000 nA before MTSR labeling, suggesting extrapolated responses of 40–200 μA to saturating doses of ACh. These currents cannot be measured accurately with our circuits; therefore, where indicated, responses were measured in low-Na recording solution.

Current and fluorescence traces were acquired at 40 Hz with an Axon Digidata interface and pCLAMP8. The fluorescence signal was filtered at 5 Hz by an eight-pole low-pass filter, then subjected to further digital filtering (1–2 Hz eight-pole Bessel) and baseline adjustment where appropriate. Waveforms were fitted to single or double exponentials with routines in ORIGIN 7 and CLAMPFIT 8. Dose–response relationships were fit to the Hill equation by using ORIGIN 7. All current and fluorescent measurements are presented as mean ± SE.

***cis*-Bis-Q Photoisomerization.** For light-flash experiments, a beam splitter (FC70, Rapp OptoElectronic) directed light from a Xe flashlamp (JML-C1, Rapp OptoElectronic, filtered by Schott GG375, BG12, and KG5, yielding 410–450 nm) and from the Hg fluorescence illuminator (with Chroma Technology HQ545/30× exciter filter) to the fluorescence cube and a 20× objective lens, N.A. 0.75. Signals were acquired at 20 kHz and then filtered at 1 kHz.

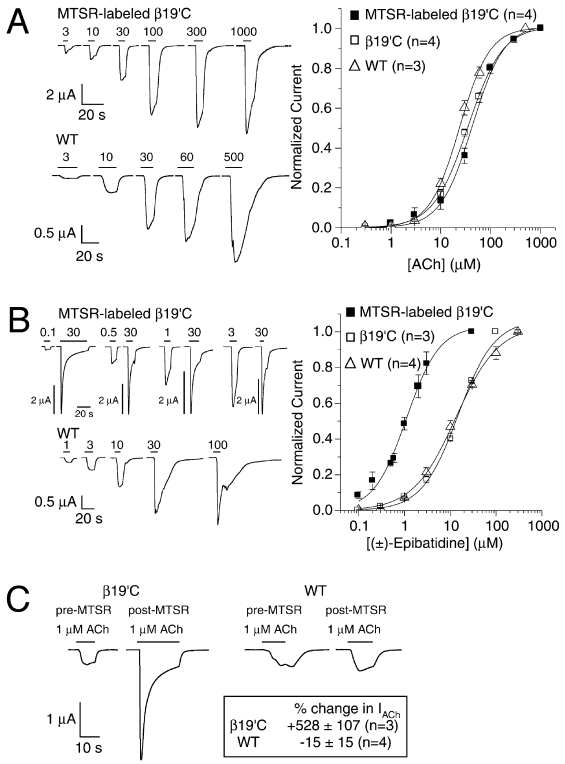

Fig. 1. Effects of MTSR labeling on nAChR electrophysiology. (*A* and *B*) Traces, dose–response relations, and fits to the Hill equation for WT-, β19′C-, or MTSR-labeled β19′C by using either ACh (*A*) or epibatidine (*B*). The bars show agonist application at the indicated concentration (μM). The epibatidine dose–response relation for MTSR-labeled β19′C was determined by administering only two doses of epibatidine to each oocyte, a single test dose (0.1–6 μM, n = 4–8 oocytes per dose), and a saturating dose (30 μM). The ACh dose–response relations were determined by administering seven to eight concentrations to each of three to four oocytes. Apart from the ACh experiments with β19′C- and MTSR-labeled β19′C, the experiments shown in *A* and *B* were completed with oocytes expressing high levels of receptor by using solutions with 20% of normal [Na] (*N*-methyl-D-glucamine substitution). (*C*) Effects of MTSR labeling on the response waveform. The response to 1 μM ACh was measured before and after labeling with 5 μM MTSR in the presence of 100 μM ACh. These experiments used normal [Na]. The box summarizes the changes in the peak I_{ACh}, calculated as $[(I_{ACh,\ preMTSR}/I_{ACh,\ postMTSR}) - 1] \times 100$.

Results

Fluorescent Labeling of βA19′C nAChR. It is convenient to renumber the amino acid sequence of M2 segments lining the nAChR channel, so that 1′ is near the cytoplasm and 20′ is near the extracellular solution (18). Ala-272 at the 19′ position of βM2 was mutated to Cys to allow modification with MTSR, a thiol-reactive fluorophore. After labeling, β19′C-injected oocytes were twice as fluorescent as uninjected or WT nAChR-injected oocytes (data not shown). ACh dose–response relations were measured for WT-expressing oocytes and for labeled and unlabeled β19′C-expressing oocytes and showed no major changes; WT, β19′C, and MTSR-modified β19′C had EC_{50}s of 24 ± 1, 35 ± 1, and 43 ± 4 μM, respectively, and Hill coefficients of 1.44 ± 0.04, 1.24 ± 0.06, and 1.36 ± 0.14, respectively (Fig. 1*A*). However, MTSR labeling did subtly alter β19′C receptor function. Measurements of the response at [ACh] ≤ 3 μM before and after labeling (Fig. 1*C*) indicated that whereas MTSR had little or no effect on the WT response (decrease of 15 ± 15%, n = 4), it enhanced the β19′C current response by 528 ± 107% (n = 3);

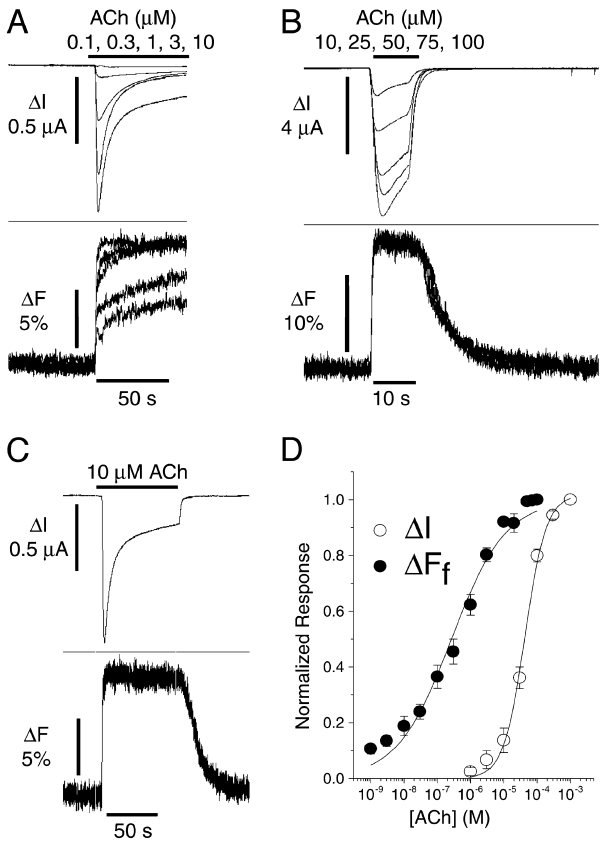

Fig. 2. ACh-induced ΔF_f occurs during a transition simultaneous with, but distinct from, channel activation. (*A*) At low [ACh], the onset of ΔF was biphasic. ACh-induced current and ΔF were recorded simultaneously at several [ACh] (traces are superimposed). The horizontal bars above the current responses indicate application of agonist. (*B*) Another oocyte. At high [agonist], the onset of ΔF was monophasic and did not correlate with channel activation. (*C*) At [ACh] $\geq$ 10 μM, there were no detectable changes in fluorescence during desensitization. (*D*) Dose–response relations and fits to the Hill equation for the peak ACh-induced current (from experiments like those of Fig. 1) and for ΔF_f, the magnitude of the fluorescence shift at the time of the peak ACh-induced current (n = 3–12 responses per dose). The dose–response relation for ΔF_f was normalized to the value for full ΔF response of a saturating dose ($\geq$10 μM ACh). [Na] was 20% of normal.

thus, the responses to 1 and 3 μM ACh were greater than the values predicted by fits of the Hill equation (Fig. 2*D*). The response waveforms before and after modification also show that MTSR modification increased the rate of β19′C desensitization.

Further indications of altered receptor function come from the dose–response relation for epibatidine. Whereas WT and β19′C had EC_{50}s of 13.1 $\pm$ 1.1 μM and 14.8 $\pm$ 1.8 μM epibatidine, respectively, the EC_{50} for MTSR-labeled β19′C was one order of magnitude lower, 1.11 $\pm$ 0.11 μM (Fig. 1*B*). The Hill coefficients showed only slight changes; WT-, β19′C-, and MTSR-labeled β19′C had Hill coefficients of 0.93 $\pm$ 0.05, 1.10 $\pm$ 0.11, and 1.22 $\pm$ 0.12, respectively. These changes in nAChR function may occur because MTSR labeling increased the affinity of the $\alpha\delta$ site for agonist (see below).

ACh-Mediated Changes in Fluorescence Intensity. Simultaneous measurements of current and fluorescence intensity indicated (Fig. 2*A*) that agonist application resulted in increased fluorescence (ΔF). Such a ΔF never occurred with control oocytes. At low doses of ACh ($\leq$10 μM), ΔF was biphasic. In bath application experiments, the faster phase (ΔF_f) was indistinguishable from the time course of the current responses, which in turn

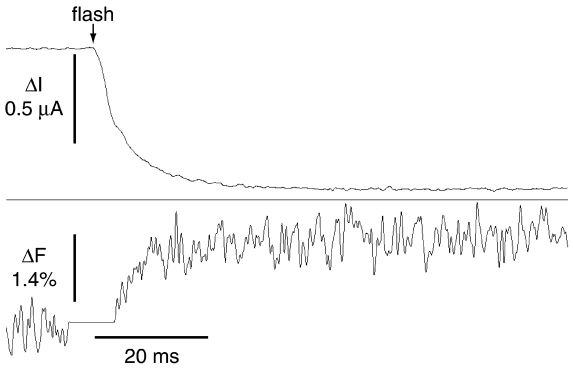

Fig. 3. Current and fluorescent responses to flash-photoisomerization of *cis*-Bis-Q. Oocytes expressing MTSR-labeled β19′C were perfused with 1 μM *cis*-Bis-Q (> 99% *cis*), eliciting a 160-nA current (data not shown); photoisomerization (a 1-ms flash $\approx$5 s after start of *cis*-BisQ perfusion) elicited a 765-nA current. Control traces were averaged from data before perfusion of *cis*-Bis-Q and after washout, then were subtracted from the trace during *cis*-Bis-Q. A shutter protecting the photomultiplier tube was closed before the flash, resulting in a $\approx$9-ms gap in the fluorescence data.

cannot be distinguished from the time course of solution change near the oocyte. The slower phase (ΔF_s) was similar to that of desensitization (Fig. 2*A*; analyzed in Fig. 5 below). At [ACh] $\geq$ 10 μM, ΔF reached its maximum magnitude (average $\Delta F/F$ $\approx$10%) and consisted of a single component that increased with the same time course as the rise of the current, with no further change in fluorescence intensity during desensitization (Fig. 2 *B* and *C*). To measure the dose–response relation of ΔF_f (Fig. 2*D*), fluorescence intensity was determined at peak current. Although ΔF_f was simultaneous with the rising phase of the current response, it clearly did not correlate with activation; with ACh, the EC_{50} for ΔF_f (266 $\pm$ 43 nM, Hill coefficient = 0.53 $\pm$ 0.04) was two orders of magnitude lower than the EC_{50} for the current response (43 $\pm$ 4 μM). Thus, ACh-mediated ΔF_f corresponds to a transition that reaches full occupancy at [ACh] much less than the EC_{50} for activation.

Photoisomerization of *cis*-Bis-Q Reveals That ΔF Is Complete Within 20 ms. We used $\approx$1-ms light flashes to jump the concentration (Fig. 3) of the photoisomerizable agonist *trans*-Bis-Q (19). The flash-induced ΔI was fitted by a single exponential with τ = 5.5 and 5.3 ms for β19′C and WT, respectively. As perfusion continued with the inactive *cis*-Bis-Q isomer, ΔI decayed (τ = 2.6–2.9 s) due to washout and diffusion of *trans*-Bis-Q as well as desensitization (data not shown). A ΔF (1.8%) was seen for β19′C (Fig. 3) but not WT-expressing oocytes (data not shown). The absolute flash-induced ΔF was comparable with ΔF for bath-applied *trans*-Bis-Q; but background fluorescence was larger, because we recorded from the vegetal pole, which is more resistant to light flashes but is also approximately five times more autofluorescent. Thus, a component of ΔF is complete within 20 ms after an agonist concentration jump, one to two orders of magnitude faster than Bis-Q-mediated desensitization.

Epibatidine-Mediated ΔF_f Corresponds to a Step Tightly Coupled to Channel Activation. Compared with ACh and carbamylcholine, epibatidine activates muscle nAChR with unique site-selectivity (10). We tested the dose–response relation of ΔF_f by using epibatidine as the agonist. To compare the current and fluorescence responses to the two agonists, individual, MTSR-labeled, β19′C-injected oocytes were perfused with a saturating dose of ACh and, after allowing for recovery, a saturating dose of epibatidine (Fig. 4*A*). Epibatidine was a partial agonist; 30 μM epibatidine (a dose 27 times greater than EC_{50}) elicited currents

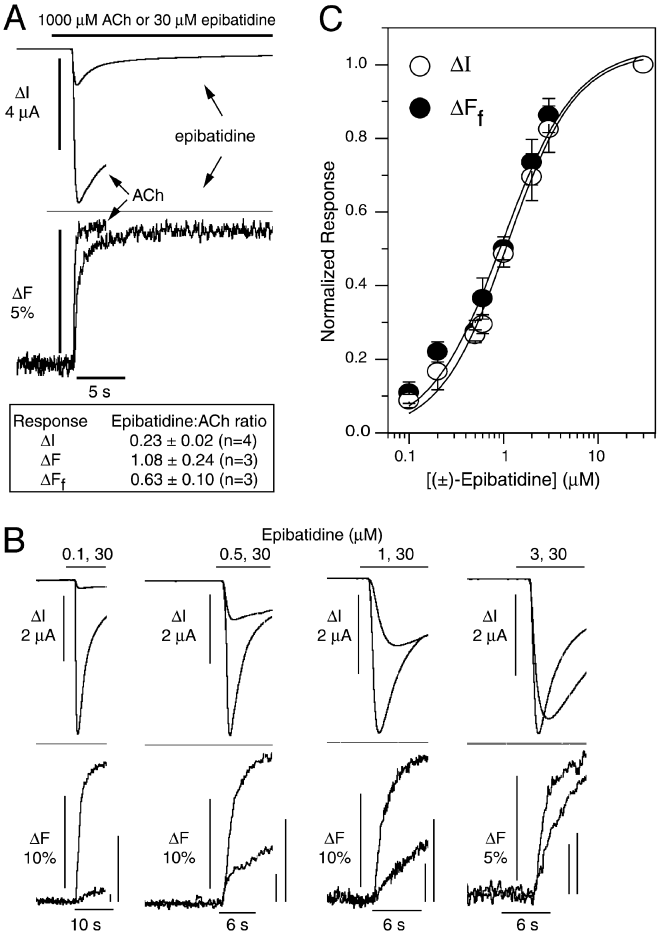

Fig. 4. Epibatidine-induced ΔF_f occurs during a transition closely linked to channel activation. (*A*) Epibatidine evokes smaller maximal currents than ACh, but a ΔF similar in magnitude. Sequential saturating doses of ACh and epibatidine were administered and the current and ΔF responses were superimposed. A representative trace is shown and the box summarizes comparisons of ACh and epibatidine induced current, ΔF, and ΔF_f. (*B*) Representative traces of current and ΔF responses to test and saturating doses of epibatidine. Bars show duration of agonist application at the indicated [epibatidine] of the test and saturating doses (μM). The vertical bars to the right of the ΔF response indicate ΔF_f magnitude. (*C*) Dose–response relations and fits to the Hill equation for epibatidine-induced current (determined as described in Fig. 1) and ΔF_f ($n = 4$–8). [Na] was 50% of normal.

from MTSR-labeled β19′C that were 0.23 ± 0.02 ($n = 4$) of that elicited by 1,000 μM ACh (a dose 23 times greater than EC_{50}). Saturating doses of both agonists, however, elicited similar increases in fluorescence intensity; the magnitude of the epibatidine ΔF was 1.08 ± 0.24 ($n = 3$) that of the ACh ΔF, suggesting that the two agonists mediate similar changes in the fluorophore environment. Interestingly, whereas ACh elicited a biphasic ΔF only at low doses, epibatidine produced a biphasic ΔF at all doses tested. At saturating doses of agonist, the epibatidine ΔF_f was only 0.63 ± 0.10 ($n = 3$) of the ACh ΔF_f. A more striking difference was in the dose–response relation for ΔF_f (Fig. 4*C*). Whereas with ACh the EC_{50} for ΔF_f and for current activation differed by two orders of magnitude, with epibatidine, the EC_{50} for ΔF_f and for current activation were indistinguishable at 0.99 ± 0.15 μM and 1.11 ± 0.11 μM, respectively. The Hill coefficient for ΔF_f was 1.13 ± 0.16.

The Slower Phase of the Fluorescence Shift Correlates with Desensitization. Time constants determined by fitting the desensitization component of the current waveform with a single exponential

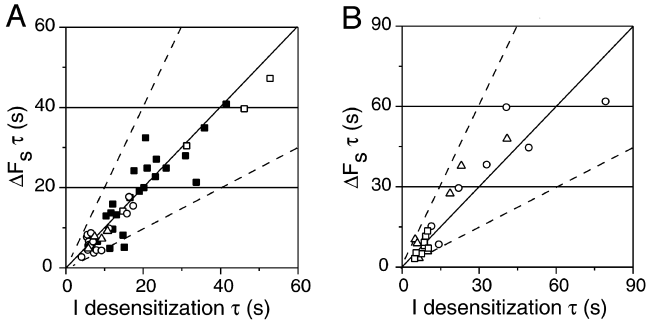

Fig. 5. Onset of ΔF_s correlates kinetically with desensitization. ACh-induced (*A*) or epibatidine-induced (*B*) ΔF responses were fit with two exponentials and the slower time constants were plotted against the time constants for desensitization. The solid and dashed lines represent equality and twofold differences, respectively. (*A*) □, 0.3 μM ($n = 4$); ■, 1 μM ($n = 25$); ○, 3 μM ($n = 17$); △, 5 μM ($n = 4$). (*B*) ○, 0.2, 0.5, and 1 μM, ($n = 7$); △, 3, 6, and 8 μM ($n = 7$); □, 10, 18, 25, and 30 μM ($n = 8$).

function were compared with the slower of the two time constants derived from fitting the entire, matching ΔF waveform with a double exponential function. Despite considerable variability in desensitization time constants, for both ACh and epibatidine (Fig. 5 *A* and *B*), there is good agreement between the time constant for ΔF_s and for current desensitization over a >20-fold range (3–70 s).

Recovery of Fluorescence Baseline Is Faster than Recovery from the Desensitized State. Upon removal of agonist the current decays faster than the fluorescence signal (Fig. 6*A*), suggesting that at least one short-lived (several seconds) desensitized state is

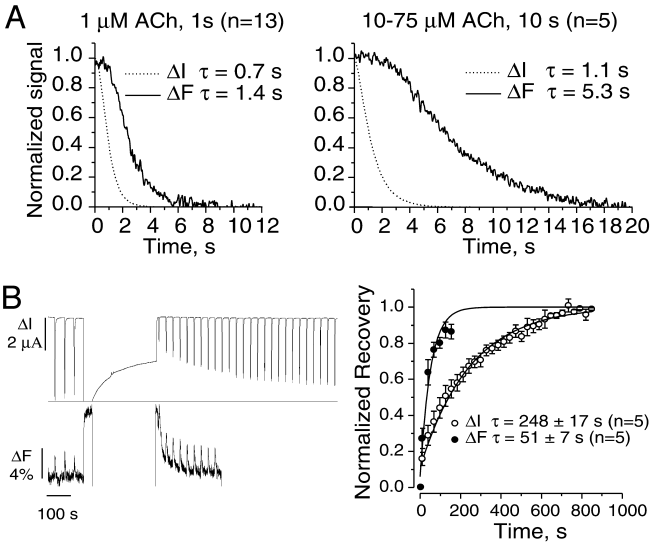

Fig. 6. Decay of ΔF after removal of agonist. (*A*) Current (dotted line) and fluorescence (solid line) decay after ACh washout was normalized and averaged. [ACh] and duration and the number of traces averaged are indicated above each trace. The traces were fitted to a single-exponential function with the indicated time constants. (*B Left*) After three 1-s test pulses of 1 μM ACh at 28-s intervals, a desensitizing step of 10 μM ACh was applied for 5 min, followed by a 10-s wash and 1-s test pulses of 1 μM ACh at 28-s intervals. To minimize photobleaching, the Hg lamp shutter was closed during the desensitizing step. A representative trace is shown. (*Right*) ○, plot of recovery of the current response after desensitization; ●, plot of return of fluorescence to baseline. Fluorescence intensity was measured just before each test pulse. The solid lines represent fits to a single exponential function with the indicated time constants.

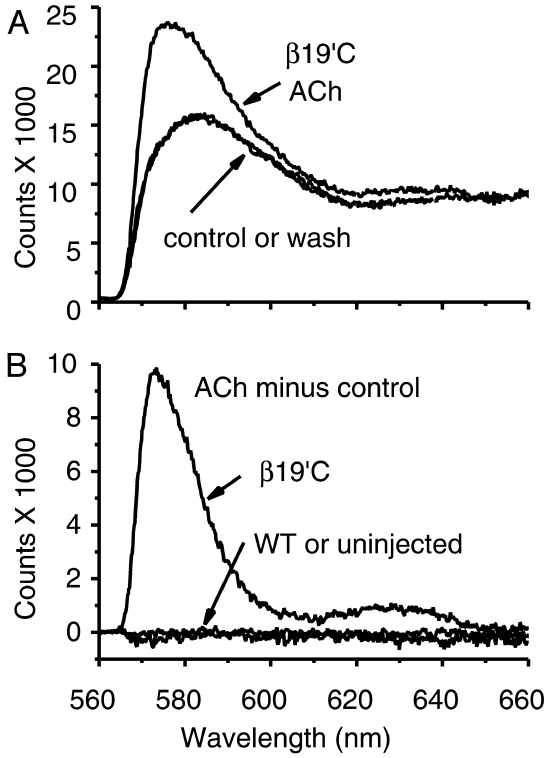

Fig. 7. Spectral analysis of MTSR-labeled oocytes. (*A*) Fluorescence spectra from an oocyte expressing β19′C receptors in the absence or presence of a desensitizing dose of ACh (500 μM for 4 min.). ACh induced a reversible leftward wavelength shift (584–574 nm) and an increase in fluorescence intensity. (*B*) Difference emission spectra from uninjected, WT-injected, or β19′C-injected oocytes. Spectra recorded in the presence of ACh were subtracted from spectra recorded in the absence of ACh. Averages of four to five cells (SEM $<$ 5% of full scale).

fluorescent. To determine whether exit from the high-fluorescence state correlates with exit from all physiologically defined desensitized states, recovery from desensitization induced by a prolonged (5-min) application of 10 μM ACh was monitored by means of brief (1-s) pulses of 1 μM ACh at 28-s intervals (Fig. 6*B*). The recovery of the fluorescence signal (●, Fig. 6*B*) is measured only approximately; but fits to a single-exponential function show a time constant several fold less than that for the recovery of the current (○, 51 ± 7 vs. 248 ± 17 s, respectively, $n = 5$). These data indicate that, upon removal of agonist, MTSR-labeled β19′C also transiently occupies at least one long-lived (several minutes) desensitized state that does not show high fluorescence.

ΔF Monitors an Increase in the Hydrophobicity of the Fluorophore's Local Environment. As solvent hydrophobicity increases, MTSR emission intensity increases and the spectrum becomes blue-shifted ($\lambda_{Ethanol} = 574$ nm; $\lambda_{ND98} = 584$ nm). In the oocyte, a desensitizing dose of ACh also increased the emission intensity and blue-shifted the emission peak by ≈10 nm (Fig. 7*A*). Therefore, ΔF occurs because the fluorophore occupies a more hydrophobic environment in the desensitized state than in the resting state, rather than because a quencher moves away (however, we cannot rule out the occurrence of both mechanisms together). There were no spectral shifts with control oocytes (Fig. 7*B*).

Discussion

In the standard kinetic scheme for nAChR activation, channel opening follows the sequential binding of agonist at the $\alpha\delta$ and

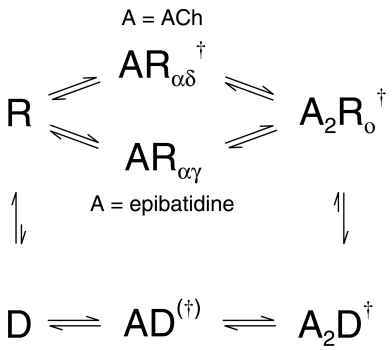

Fig. 8. Kinetic scheme accounting for ΔF seen with ACh and epibatidine. ΔF is caused by conformational changes due to productive binding of agonist to the $\alpha\delta$ site. Because ACh and epibatidine show reverse-site selectivity for the $\alpha\delta$- and $\alpha\gamma$-binding sites, the state changes follow distinct pathways, labeled A = ACh and A = epibatidine, favored by increasing concentrations of the respective agonists. With ACh, ΔF is due to formation of $AR_{\alpha\delta}$; with epibatidine, ΔF is due to formation of A_2R_o. R is the activatable receptor, A is the agonist molecule, R_o is the open receptor, and D is the desensitized receptor. $\alpha\delta$ and $\alpha\gamma$ subscripts identify binding sites occupied by ligand. A dagger (†) indicates a high-fluorescence state and a bracketed dagger an uncertain assignment. Some states are in equilibrium with counterparts that have not undergone conformational changes (not shown, for simplicity), accounting for partial agonism.

$\alpha\gamma$ sites. By using a fluorophore attached to the extracellular end of nAChR M2, we detected one of the several agonist-induced transitions. Which transition was detected?

A Scheme for the Observations. Fig. 8 shows a model that rationalizes our observations. In this scheme, a dagger (†) indicates a high fluorescence state, and all † states are assumed to be equally fluorescent. Both ΔF_f and ΔF_s occur when the fluorophore senses a conformational change due to productive binding of agonist to the $\alpha\delta$ site. Because the $\alpha\delta$ site is the high-affinity site for ACh but the low-affinity site for epibatidine, these two agonists are predicted to induce ΔF at different regions of the dose–response relation for agonist-induced currents.

This model accounts for many properties of the ΔF response. Because ACh has 30 times higher affinity for the $\alpha\delta$ site (8), $AR_{\alpha\delta}{}^{\dagger}$ is fully occupied at [ACh] much lower than required for fully occupying $A_2R_O{}^{\dagger}$. Assuming the MTSR labeling does not markedly change the site selectivity of ACh and epibatidine, this hypothesis explains how ACh EC_{50} for ΔF and for ΔI differ by a factor of 160.

Epibatidine has reverse-site selectivity. Thus, epibatidine binding to the $\alpha\delta$ site occurs predominately during formation of $A_2R_O{}^{\dagger}$, explaining why the EC_{50} for ΔF and for ΔI are indistinguishable with epibatidine.

What is the explanation for ΔF_s? With ACh, ΔF_s appears only at agonist concentrations too low to saturate the $\alpha\delta$ site. Under these conditions, ΔF_s represents equilibration among the various comparably fluorescent $R^{\dagger}$ states. More slowly, receptors enter the slow-onset-desensitized $A_2D^{\dagger}$ state(s), pulling the entire equilibrium to the right, and increasing the overall population of $R^{\dagger}$ states with a time constant equal to that of desensitization. Thus, the time constants are equal for ΔF_s and current desensitization, not because the open and desensitized states differ in fluorescence, but because the desensitized state(s) is one of the fluorescent states and because desensitization is the rate-limiting step for the equilibration, seen at low agonist dose, of the various $R^{\dagger}$ states. That flash-activation of *trans*-Bis-Q produces ΔF within 20 ms, much faster than desensitization, argues decisively against a major role for even fast desensitization as the transition that increases fluorescence.

With epibatidine, ΔF_s appears at all concentrations tested. We propose that this arises because epibatidine is a partial agonist (Fig. 4*A*); i.e., producing a limited population of receptors in the $A_2R_O^\dagger$ state. Therefore, the absolute flux from $A_2R_O^\dagger$ to $A_2D^\dagger$ is a rate-limiting step in the increase of the fluorescent receptor population, even at saturating epibatidine concentration. Interestingly, epibatidine shows different efficacies for evoking current and ΔF_f, suggesting that it may bind more productively at the $\alpha\delta$ site than at the $\alpha\gamma$ site (see discussion of sequential conformational changes below). Data for additional partial agonists and antagonists will test this proposal.

The cyclical model for desensitization (7, 20, 21) incorporated in Fig. 8 proposes that after releasing agonist, the receptor remains functionally desensitized. Upon removal of a deeply desensitizing dose of ACh, MTSR-labeled β19′C returned to the low-fluorescence state faster than functional recovery (Fig. 6), suggesting the existence of a low-fluorescence-desensitized state. In contrast to the resting state, ACh has little or no site-selectivity for the ligand-binding sites of the desensitized receptor (11, 22), and so agonist is released from the two sites at similar rates. This finding suggests that low-fluorescence-desensitized receptors are predominantly in the agonist-free desensitized state rather than the monoliganded-desensitized state.

Structural Basis of the Fluorescence Change. In *Torpedo* nicotinic receptors, the 19′ residues are nine residues and 10–14 Å from the extracellular end of M2 (4). A fluorophore tethered to β19′C would be ≈35 Å from the ligand-binding site (23) and therefore unlikely to monitor simple occupancy of the site. Although it is possible that ΔF is due solely to rearrangement of the N-terminal ligand-binding domain, the authors (4) of an electron microscopic structure suggested the presence of a conformational change that accounts for ΔF. In the resting state, the five M2 helices are separated by a water-filled space from the outer protein wall formed by the M1, M3, and M4 helices. During gating, the suggested rotation of M2 moves the 19′ residue closer to hydrophobic side chains in these other helices (4), leading to the increase in fluorescence intensity and the blue shift in the emission spectrum reported here. Presumably, ligand binding at the $\alpha\delta$ interface leads to conformational changes of their respective M2 helices as well as of the βM2 helix.

Gating Involves Sequential Conformational Changes. Because receptors in the nAChR family (*i*) are (pseudo)symmetric multimers, (*ii*) have ligand-binding sites ≈50 Å from the channel gate, and (*iii*) display supralinear dose–response relations, models of receptor function have been strongly influenced by ideas about cooperative transitions in multisubunit regulatory proteins (24, 25). In the concerted model, positive cooperativity arises because sites on the same receptor are conformationally coupled. In contrast, sequential models (26) propose that each binding site changes its conformation upon agonist binding, with positive cooperativity arising from the influence of this transition on the neighboring binding site. With one ligand bound the receptor adopts an intermediate state between resting and open.

This paper provides a way to define states of the nAChR. Our present simultaneous electrophysiology and fluorescence measurements indicate that the fluorophore detects conformational changes in or around βM2 after agonist binding at the $\alpha\delta$ interface. At low [ACh], we detected an intermediate state comprising an $\alpha\delta$ site in the active conformation and an $\alpha\gamma$ site in the resting conformation, as revealed by the strong fluorescence response and weak current response. At low [epibatidine], the major monoliganded intermediate state involves the $\alpha\gamma$ site, which is not fluorescent. The straightforward interpretation of these results is that in the MTSR-modified nAChR, subunits undergo sequential rather than fully concerted transitions.

Fluorescent labeling of other nAChR residues and other subunits may permit further detection and characterization of conformational changes associated with movement of the channel gate during activation and desensitization. In conjunction with structural studies, such knowledge will enhance our understanding of the structural transitions occurring during allosterically controlled channel gating.

We thank A. Karlin for providing the βA19′C mutant and K. Kostenko and S. Kwoh for assistance with oocytes. This work was supported by National Institutes of Health Grants NS-11756, NS-34407, and GM-30376, and by a fellowship from the American Heart Association (to B.C.).

1. Miyazawa, A., Fujiyoshi, Y., Stowell, M. & Unwin, N. (1999) *J. Mol. Biol.* **288,** 765–786.
2. Karlin, A., Holtzman, E., Yodh, N., Lobel, P., Wall, J. & Hainfeld, J. (1983) *J. Biol. Chem.* **258,** 6678–6681.
3. Brejc, K., van Dijk, W. J., Klaassen, R. V., Schuurmans, M., van Der Oost, J., Smit, A. B. & Sixma, T. K. (2001) *Nature* **411,** 269–276.
4. Miyazawa, A., Fujiyoshi, Y. & Unwin, N. (2003) *Nature* **424,** 949–955.
5. Karlin, A. (2002) *Nat. Rev. Neurosci.* **3,** 102–114.
6. Changeux, J. P. & Edelstein, S. J. (1998) *Neuron* **21,** 959–980.
7. Katz, B. & Thesleff, S. (1957) *J. Physiol. (London)* **138,** 63–80.
8. Zhang, Y., Chen, J. & Auerbach, A. (1995) *J. Physiol. (London)* **486,** 189–206.
9. Blount, P. & Merlie, J. P. (1989) *Neuron* **3,** 349–357.
10. Prince, R. J. & Sine, S. M. (1998) *Biophys. J.* **75,** 1817–1827.
11. Sine, S. M. & Claudio, T. (1991) *J. Biol. Chem.* **266,** 19369–19377.
12. Chang, Y. & Weiss, D. S. (2002) *Nat. Neurosci.* **5,** 1163–1168.
13. Nerbonne, J. M., Sheridan, R. E., Chabala, L. D. & Lester, H. A. (1983) *Mol. Pharmacol.* **23,** 344–349.
14. Quick, M. & Lester, H. A. (1994) in *Ion Channels of Excitable Cells*, ed. Narahashi, T. (Academic, San Diego), pp. 261–279.
15. Zhang, H. & Karlin, A. (1998) *Biochemistry* **37,** 7952–7964.
16. Cha, A. & Bezanilla, F. (1998) *J. Gen. Physiol.* **112,** 391–408.
17. Li, M., Farley, R. A. & Lester, H. A. (2000) *J. Gen. Physiol.* **115,** 491–508.
18. Hille, B. (2001) *Ion Channels of Excitable Membranes* (Sinauer, Sunderland, MA).
19. Lester, H. A. & Nerbonne, J. M. (1982) *Annu. Rev. Biophys. Bioeng.* **11,** 151–175.
20. Rang, H. P. & Ritter, J. M. (1970) *Mol. Pharmacol.* **6,** 357–382.
21. Chang, Y., Ghansah, E., Chen, Y., Ye, J. & Weiss, D. S. (2002) *J. Neurosci.* **22,** 7982–7990.
22. Sine, S. M., Ohno, K., Bouzat, C., Auerbach, A., Milone, M., Pruitt, J. N. & Engel, A. G. (1995) *Neuron* **15,** 229–239.
23. Unwin, N. (2003) *FEBS Lett.* **555,** 91–95.
24. Jackson, M. B. (1994) *Trends Biochem. Sci.* **19,** 396–399.
25. Karpen, J. W. & Ruiz, M. (2002) *Trends Biochem. Sci.* **27,** 402–409.
26. Koshland, D. E., Jr., Nemethy, G. & Filmer, D. (1966) *Biochemistry* **5,** 365–385.